Journal Name

ARTICLE

Reflux precipitation polymerization: a new synthetic insight in molecular imprinting at high temperature

Xiantao Shen,*[abd] Chuixiu Huang,*[bcd] Sudhirkumar Shinde,[b] Magdalena Switnicka-Plak,[e] Peter Cormack[e] and Börje Sellergren*[b]

Synthesis of uniform molecularly imprinted polymer (MIP) microspheres (MSs) using distillation precipitation polymerization (DPP) at high temperature has attracted great interest in the field of molecular imprinting. However,there were still some shortcomings in this method. In this work, to create uniform MIP MSs in a short time and to demonstrate the effects of high temperature on imprinting performance, a new precipitation polymerization method (reflux precipitation polymerization, RPP) was used for the first time to fabricate MIP MSs in this study. The SEM images of the polymeric MSs indicate the presence of template molecules could improve the particle morphology and size uniformity. The specific molecular recognition of the monodispersed MIP MSs was confirmed by fluorescence measurement and HPLC-UV analysis. The binding behavior of the MIP MSs was simulated using the heterogeneous Freundlich isotherm, which shows that the MIP MSs produced by the RPP possess compatible selectivity in comparison with those by traditional PP method. It is noted that, for the first time, we demonstrated that molecular imprinting at high temperature was only successful when electrostatic interactions played important roles in the imprinting process.

1. Introduction

Molecularly imprinted polymers (MIPs), which are also named synthetic receptors or artificial antibodies, are cross-linked polymers with well-defined binding sites.[1,2] During the synthesis process, the specific binding cavities were usually created by employing a molecular template.[3,4] So far MIPs have become interesting materials in the field of separation, chemical sensors and biosensors, catalysis and drug delivery.[5,6]

Up to date, several different methods have been reported for the synthesis of MIPs, which include bulk polymerization, precipitation polymerization (PP), surface imprinting polymerization, suspension polymerization, Pickering emulsion polymerization and so on.[7,8] Among these methods, PP is one of the most popular approach for the preparation of MIP spherical particles without the presence of surfactants.[9,10]

Because the MIP microspheres (MSs) generated by PP are more uniform in size and offer higher active surface area, this kind of MSs showed great potential in reproducible chromatography analysis and sensors.[11,12]

The progress of molecular imprinting *via* PP involves template-monomer complex formation, particle nucleation, ordered particle growth and coagulation of beads. Therefore, the solvent should be a good solvent for the monomers to facilitate the formation of the complex with template molecule, but a poor solvent for the MIP particles to facilitate the precipitation of particles.[13,14] In particle nucleation phase, the formation of the complex between the function groups of the monomers and the template molecule can be described. As a consequence, monodispersed MIP MSs can be produced in well-controlled conditions.[15] However, long polymerization time (e.g. 24 h) was usually required for traditional PP with a reaction temperature of approximately 60 °C, therefore new methods for the synthesis of uniform MIP particles in a relatively short time are attractive.[16]

To shorten the polymerization time, an improved PP (named distillation precipitation polymerization, DPP) has been introduced in molecular imprinting.[17,18] DPP was developed in 2004 to synthesize uniform MSs in a more efficient way (within 3 h).[19] The polymerization was performed in neat acetonitrile (ACN) under reflex condition, and some of ACN was distilled off during the polymerization process to accelerate the precipitation of the cross-linked polymers.[20,21] In 2009, DPP was first employed for the preparation of MIP particles by Yang and co-workers, where MIP nanoparticles were synthesized in 3 hours by DPP. Recently, core-shell

[a.] Key Laboratory of Environment and Health, Ministry of Education & Ministry of Environmental Protection, State Key Laboratory of Environmental Health (Incubation), School of Public Health, Tongji Medical College, Huazhong University of Science and Technology, Hangkong Road #13, Wuhan, Hubei 430030, China. E-mail: xtshenlab@hust.edu.cn
[b.] Department of Biomedical Sciences, Faculty of Health and Society, Malmö University, SE20506 Malmö, Sweden. E-mail: borje.sellergren@mah.se
[c.] School of Pharmacy, University of Oslo, PO Box 1068 Blindern, 0316 Oslo, Norway. E-mail: chuixiuh@student.matnat.uio.no
[d.] G&T Septech AS, Verkstedveien 29, 1400 Ski, Norway
[e.] Department of Pure & Applied Chemistry, University of Strathclyde, Thomas Graham Building, 295 Cathedral Street, Glasgow, G1 1XL, UK
† Electronic supplementary information (ESI) available: Macroscopic images of the microspheres; simulation for adsorption of propranolol using Freundlich model. See DOI: 10.1039/x0xx00000x

hydrophilic MIP nanoparticles were prepared successfully with DPP method.[22] Most recently, Wang et al. reported that a type of thermosensitive hairy hollow imprinted MSs by combining DPP and click chemistry.[23]

The application of DPP in MIP technique shows that synthesis of MIPs at high temperature can reduce the synthesis time significantly but without influence the molecular recognition ability of MIPs.[24] However, DPP could cause unstable polymerization and notable loss of particles on the wall of the container because of the distillation of some solvent gradually. [25] It might be due to the unstable polymerization, DPP was often used to construct thin imprinted layers on the non-imprinted nanoparticles or hollow imprinted shells in the literature.[26,27]

To overcome the limitations of PP and DPP, other synthetic methods are emergently needed to prepare MIP MSs with uniform cavities in a short time. Recently, a modified DPP method was developed by Wang and the co-workers to produce MSs (without molecular imprinting concept), where the apparatus for the receiving of the distilled solvent was replaced with a condenser.[28] This method was named reflux precipitation polymerization (RPP). With this RPP method, uniform MSs were obtained within a short time. In comparison with traditional PP and DPP, RPP is an idea platform for the synthesis of uniform cross-linked polymer beads[29,30] or core-shell MSs.[31,32] In this paper, RPP was used to generate uniform MIP MSs. The polymerization is carried out under the reflux condition at a high temperature, so the volume of the solvent during the polymerization is constant, which will result in a stable polymerization. To the best of our knowledge, this is the first generation of uniform MIP MSs using RPP in a short time to be reported and also the first demonstration of the main interactions in molecular imprinting at high temperature. We believe this RPP synthetic methodology will provide new insights in molecular imprinting.

2. Experimental methods

2.1 Materials

2,2-Azobisisobutyronitrile (AIBN, 98%) and 2,2'-azobis(2,4-dimethylvaleronitrile) (ABDV, 98%) were purchased from Merck (Darmstadt, Germany). Methacrylic acid (MAA, 98.5%) was purchased from Sigma-Aldrich (Deisenhofen, Germany). Divinylbenzene (DVB, 80%, technical grade, mixture of isomers) was purchased from Sigma-Aldrich (Deisenhofen, Germany). (R,S)-propranolol hydrochloride (99%), oxprenolol (99%), alprenolol (99%), 1-naphthol (99%) and 1-naphthylamine (99%) were supplied by Sigma-Aldrich (Deisenhofen, Germany). HPLC grade acetonitrile (ACN), methanol, citric acid monohydrate and sodium citrate tribasic dihydrate were purchased from Merck (Darmstadt, Germany). (R,S)-propranolol hydrochloride was transferred to free base when it was used as template molecules. AIBN was recrystallized from methanol before use. Polymerization inhibitors in DVB were removed by passing it through an

aluminum oxide column prior to use. Other solvents were used without further purification.

2.2 Synthesis of MIP and NIP MSs by RPP

In molecular imprinting, both ethylene glycol dimethacrylate (EGDMA) and DVB were usually used as crosslinking monomers. In comparison with EGDMA, DVB was more suitable for synthesis of uniform MIP MSs using precipitation polymerization.[9,33] Therefore, in this work we selected DVB as the crosslinking monomer.

The experimental setup of RPP has been described elsewhere by Wang et al.[28] To produce MIP MSs, 130 mg of (R,S)-propranolol, 300 μL of MAA, 1200 μL of DVB, and 28 mg of AIBN were dissolved in 40 mL of ACN in a round-bottom bottle. After purging with nitrogen for 5 min, the round-bottom bottle was equipped with a condenser and placed into a 90 ℃ oil bath to induce the polymerization. After the reaction, the MSs were collected by centrifugation. To remove the template, the polymeric MSs were washed with methanol containing 10% acetic acid. The concentration of propranolol in the washing solvent was measured with a Fluorescence Reader (Gemini EM Microplate Reader, California). When no template could be found in the washing solvent, the polymeric MSs were washed with ACN, and dried in a vacuum chamber at room temperature. In such a way, the MIP MSs were synthesized and named mip-RPP MSs. As a control, nip-RPP MSs were also prepared without the addition of the template under the same condition for the synthesis of mip-RPP MSs.

2.3 Synthesis of MIP and NIP microspheres by PP

As a reference, MIP MSs were also prepared using traditional PP as reported.[34] Typically, 65 mg of (R,S)-propranolol was dissolved in 20 mL of ACN in a borosilicate glass tube with a screw cap. Afterwards, 150 μL of MAA, 600 μL of DVB and 14 mg of ABDV were added. The solution was purged with nitrogen for 5 min and sealed. Subsequently, the polymerization was initiated by placing the glass reactor into a 60 ℃ water bath, and the polymerization was kept for 24 h. After the reaction, the MSs were collected by centrifugation. To remove the template, the polymeric MSs were washed with methanol containing 10% acetic acid. The concentration of propranolol in the washing solvent was measured with a Fluorescence Reader. When no template could be found in the washing solvent, the polymeric MSs were washed with ACN, and dried in a vacuum chamber at room temperature. In this way, the MIP MSs were synthesized and named mip-PP MSs. As a control, nip-PP MSs were also prepared without the addition of the template under the same condition as that for the synthesis of mip-PP MSs.

2.4 Synthesis of MIP and NIP MSs by DPP

The mip-DPP and nip-DPP MSs were synthesized *via* DPP in a round-bottom flask connected to a Dean-Stark receiver.[22] Briefly, 130 mg of (R,S)-propranolol, 300 μL of MAA, 1200 μL of DVB and 28 mg of AIBN were dissolved in 40 mL of ACN in a round-bottom bottle. After purging with nitrogen for 5 min, the flask was connected to the Dean-Stark receiver. With an oil

bath, the reaction system was heated to 80 ℃ for 20 min under stirring. In 30 min, the oil bath temperature was increased to 115 ℃. Thereafter, 20 mL of ACN was removed in 2 h through the Dean-Stark receiver. After the reaction, the MSs were collected by centrifugation. To remove the template, the polymeric MSs were washed with methanol containing 10% acetic acid. The concentration of propranolol in the washing solvent was measured with a Fluorescence Reader (Gemini EM Microplate Reader, California). When no template could be found in the washing solvent, the polymeric MSs were washed with ACN, and dried in a vacuum chamber at room temperature. In such a way, the MIP MSs were synthesized and named mip-DPP MSs. As a control, nip-DPP MSs were also prepared without the addition of the template under the same condition for the synthesis of mip-DPP MSs.

2.5 Synthesis of 17β-estradiol (E2) imprinted MSs

To study the effects of high temperature on molecular imprinting, E2 imprinted MIP MSs were also prepared using both PP and RPP. Typically, 130 mg of E2 was dissolved in 20 mL of ACN in a borosilicate glass tube with a screw cap. Afterwards, 150 µL of MAA, 600 µL of DVB and 14 mg of ABDV were added. The solution was purged with nitrogen for 5 min and sealed. Subsequently, the polymerization was initiated by placing the glass reactor into a 60 ℃ water bath, and the polymerization was kept for 24 h. After the reaction, the MSs were collected by centrifugation. To remove the template, the polymeric MSs were washed with methanol and ACN. The concentration of E2 in the washing solvent was measured with a Fluorescence Reader (λ_{ex} = 280 nm, λ_{em} = 306 nm). When no template could be found in the washing solvent, the polymeric MSs were washed with ACN, and dried in a vacuum chamber at room temperature. In this way, the MIP MSs were synthesized and named E2-mip-PP MSs. As a control, E2-nip-PP MSs were also prepared without the addition of the template under the same condition as that for the synthesis of E2-mip-PP MSs.

To produce MIP MSs using RPP method, 130 mg of E2, 150 µL of MAA, 600 µL of DVB and 14 mg of AIBN were dissolved in 20 mL of ACN in a round-bottom bottle. After purging with nitrogen for 5 min, the round-bottom bottle was equipped with a condenser and placed into a 90 ℃ oil bath to induce the polymerization. After the reaction, the MSs were collected by centrifugation. To remove the template, the polymeric MSs were washed with methanol containing 10% acetic acid. The concentration of E2 in the washing solvent was measured with a Fluorescence Reader (λ_{ex} = 280 nm, λ_{em} = 306 nm). When no template could be found in the washing solvent, the polymeric MSs were washed with ACN, and dried in a vacuum chamber at room temperature. In such a way, the MIP MSs were synthesized and named E2-mip-RPP MSs. As a control, E2-nip-RPP MSs were also prepared without the addition of the template under the same condition for the synthesis of E2-mip-RPP MSs.

2.6 Characterization

The images of the polymeric MIP/NIP MSs synthesized with different conditions were recorded by an inverted optical microscope with HMX lamphouse assembly (model TMS-F) made by Nikon Japan. The surface morphology for the mip-RPP MSs was observed by scanning electron microscope (SEM) on a Thermal Field Emission SEM LEO 1560 instrument (Zeiss, Oberkochen, Germany).

The surface groups of the imprinted MSs were investigated by attenuated total reflection (ATR) Fourier transform infrared spectrometry (FTIR) analysis on a Nicolet iS5 FTIR Spectrophotometer (Thermo Scientific). All spectra were recorded at room temperature in the region of 4000-375 cm^{-1} with a resolution of 4 cm^{-1} using 16 scans.

The size of MIP/NIP MSs was measured using dynamic light scattering (DLS) at 25 ℃ on a Zetasizer Nano ZS instrument equipped with a software package DTS Ver. 4.10 (Malvern Instruments Ltd., Worcestershire, UK).

2.7 Equilibrium binding profile

Previous works indicated that a mixture of 25 mM citrate buffer (pH 6) and ACN (50/50, v/v) was a proper solvent in the binding test of propranolol on MAA based MIPs.[10,35] Therefore, to investigate the binding capacity of the polymeric MSs synthesized in this work, 1 mL of propranolol solution, which is a mixture of 25 mM citrate buffer (pH 6) and ACN (50/50, v/v) with various concentrations of propranolol, was added into a series of 1.5 mL Eppendorf tubes containing 5 mg of polymeric MSs. The mixture was incubated at room temperature for 16 h. After centrifugation, the supernatant (200 µL) was collected and measured using a fluorescence reader. The fluorescence intensity of propranolol was measured with λ_{ex}=278 nm and λ_{em}=356 nm, respectively. It is noted that the linearity range for the analysis were 1-20 mg L^{-1} (r^2=0.94). When propranolol concentration is higher than 20 mg L^{-1}, the sample is diluted with a mixture of 25 mM citrate buffer (pH 6) and ACN (50/50, v/v) before testing. The amount of propranolol bound to the MSs was calculated from the reduction of the fluorescence intensity in comparison with the reference solution, and the equilibrium adsorption capacity (q_e, mg g^{-1}) of the MSs is calculated using the following equation:

$$q_e = \frac{(C_0 - C_e) \cdot v}{m} \quad (1)$$

where C_e and C_0 are the equilibrium concentration of propranolol (mg mL^{-1}) in the supernatant after the adsorption and the initial concentration of propranolol (µg mL^{-1}) in the solution before the adsorption, respectively. v and m are the volume of propranolol solution (1 mL) and the mass of the MSs (5 mg), respectively.

2.8 Kinetic binding profile

To investigate the binding kinetics of the polymeric MSs, 1 mL of 67 µmol (20 ppm) propranolol solution in a mixture of 25 mM citrate buffer (pH 6) and ACN (50/50, v/v) was added into a series of 1.5 mL Eppendorf tubes containing 5 mg of polymeric MSs. Subsequently, the mixtures were stirred and incubated for a desired time (from 5 to 300 min) at room

temperature. After the incubation, immediately, the mixture was centrifuged, and the supernatant was collected for the measurement by fluorescence reader.

2.9 Selectivity study

To evaluate the selectivity of MIP particles, oxprenolol, alprenolol, 1-naphthol and 1-naphthylamine were selected as control compounds, which possess similar structure as that of the template propranolol as shown in Fig. S1. Typically, 1 mL of various compounds with a concentration of 67 µM (single or a mixture with propranolol) in a mixture solution of 25 mM citrate buffer (pH 6) and ACN (50/50, v/v) was added into a series of 1.5 mL Eppendorf tubes containing 5 mg of polymeric MSs. The mixture was incubated at room temperature overnight. After the incubation, the supernatant was collected for measurement.

Table 1. Size distribution, the yield and the uptake of propranolol by the polymeric MSs synthesized with different conditions.

Entry	Method	Time (h)	MIP MSs			NIP MSs		
			Size ^{a} (µm)	Yield (%)	Uptake (%)	Size ^{a} (µm)	Yield (%)	Uptake (%)
1	RPP	0.25	0.6±0.3	1.6	65.9	0.4±0.4	1.3	24.5
2	RPP	0.5	1.1±0.3	6.0	73.0	0.7±0.3	6.6	23.2
3	RPP	1	1.4±0.2	13.5	71.3	0.8±0.3	12.9	21.4
4	RPP	2	2.0±0.2	33.7	72.9	1.1±0.2	29.1	21.6
5	RPP	3	2.1±0.2	45.8	78.4	1.2±0.2	38.7	19.5
6	RPP	4	2.4±0.3	58.1	79.1	1.3±0.2	62.0	26.0
7	PP	24	1.8±0.3	32.4	71.4	1.4±0.2	37.1	14.2
8	DPP	3	3.3±0.4 10.1±8.5	30.3	73.6	4.9±1.7 26.4±13.4	32.5	10.8

^{a} The mip-DPP and nip-DPP MSs showed polydispersity in size distribution because of the unstable polymerization.

The uptake of single 1-naphthol and 1-naphthylamine by MIP/NIP MSs was measured using a fluorescence reader. Typically, 200 µL of the supernatant was added into the 96 well quartz plate (Hellma Analytics, Germany). When the quartz plate was placed into the fluorescence reader, the fluorescence intensity was measured using the following parameters: 1-naphthol, λ_{ex} = 293 nm, λ_{em} = 352 nm; 1-naphthylamine, λ_{ex} = 313 nm, λ_{em} = 428 nm. Other single compounds (oxprenolol and alprenolol) and the binary mixture compounds were determined by HPLC-UV analysis (Dionex Ultimate 3000 system equipped with a VWD-3400 UV/VIS detector from Dionex Corporation, Sunnyvale, CA, USA). The separation was performed on a Gemini C18 column (150 mm X 2.00 mm, 5 µm). The UV detection wavelength was selected at 214 nm, and the injection volume was 10 µL. Mobile phase A was 20 mM formic acid (in water) containing 5% ACN, and mobile phase B was ACN containing 5% 20 mM formic acid. The gradient was shown as follows: 0-15 min, 0-30% (phase B); 15-15.1 min, 30-80% (phase B); 15.1-17 min, 80% (phase B); 17-17.1 min, 80-0% (phase B); 17.1-20 min, 0% (phase B). The flow rate was 0.4 mL min^{-1}.

3. Results and discussion

3.1 Materials synthesis and characterization

Polymerization time is an important factor influencing the size and uniformity of the MSs.[36,37] To investigate the effect of polymerization time on the mip-RPP MSs, different polymerization time from 15 min to 4 hours were conducted. The size distribution of the mip-RPP MSs *via* DLS analysis synthesized using various time are shown in Table 1. It is clear that the size of the MSs increases with increasing the polymerization time. As a consequence, longer polymerization time resulted in higher yield and larger particle in size (Table 1 and Fig. S5). However, longer polymerization time somewhat deteriorated the uniformity as shown in Table 1, which is consistent with previous observations.[38] According to the observations above, 2 hours was selected as the optimal reaction time for the synthesis of uniform mip-RPP MSs.
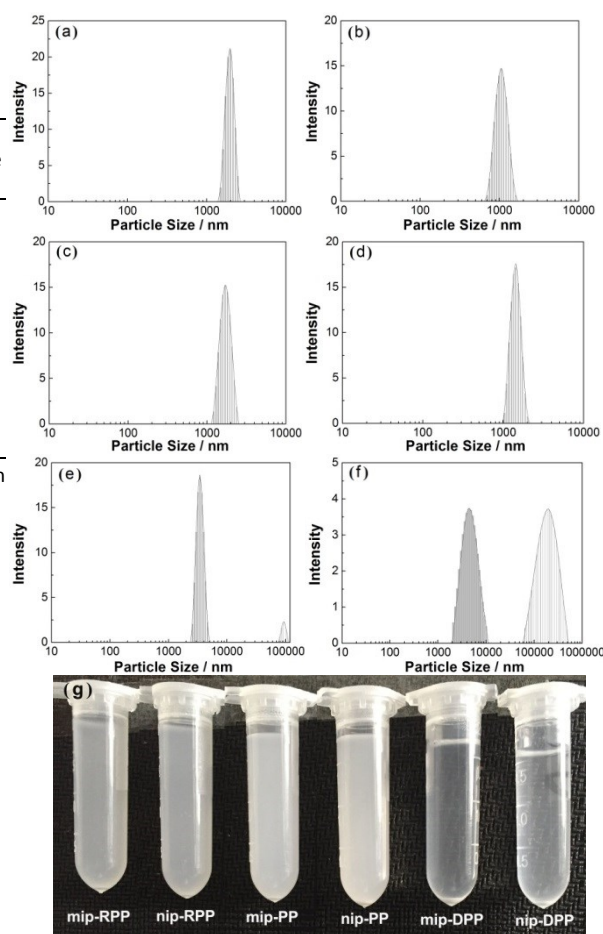

Fig. 1 Size distributions of polymeric microspheres measured by DLS: (a) mip-RPP MSs, (b) nip-RPP MSs, (c) mip-PP MSs, (d) nip-PP MSs, (e) mip-DPP MSs, (f) nip-DPP MSs. (g) Macroscopic view of the MSs (1 mg) dispersed in ACN (2 mL) after a 30-min stewing period.

The DLS analysis of mip-RPP and nip-RPP MSs are presented in Fig. 1. It is demonstrated that the mip-RPP MSs were quite uniform with a diameter of 2.0±0.2 µm. This finding was proved by the SEM measurement (Fig. 2). However, the size distribution of nip-RPP MSs was in the range of 1.1±0.2 µm (Fig. 1b). Interestingly, the optical microscope images in Fig. S8 and the SEM image in Fig. S9 showed that the morphology of nip-RPP MSs were non-uniform (from 0.5 µm to 2 µm). The

results indicate the addition of propranolol influenced the particle uniformity and size distribution of the imprinted polymers. This improvement of the MIP morphology by adding propranolol is in agreement with a previous work reported by Chen et al.[39]
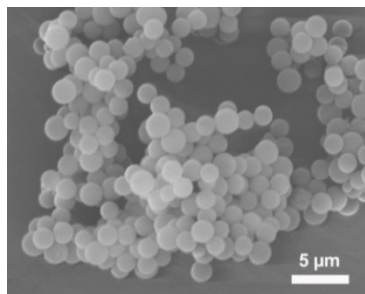

Fig. 2 SEM images of mip-RPP MSs.

As references, mip-PP MSs (or nip-PP MSs) and mip-DPP MSs (or nip-DPP MSs) were also prepared using traditional PP at lower temperature (60 °C) and using DPP under reflex condition, respectively. It is clear in Table 1 that the yields of both MIP and NIP MSs by RPP for 2 hours, DPP for 3 hours and PP for 24 hours are comparable. Moreover, the equilibrium binding ability of MSs produced by RPP, DPP and PP does not show significant difference for both MIP and NIP MSs (Table 1). The size distribution of the polymeric MSs is shown in Fig. 1. It is clear that the MSs produced by RPP and PP were monodispersed, whereas the MSs produced by DPP were polydispersed because of the aggregation (unstable polymerization). This character of the mip-DPP MSs was confirmed in Fig. 1e and Fig. S6. In addition, Fig. S2 shows that DPP could cause notable loss of the mip-DPP MSs on the wall of the flask because of the distillation off some solvent gradually.

The surface group of mip-RPP, mip-PP and mip-DPP MSs was characterized using FT-IR. The mip-RPP and mip-DPP MSs showed the same spectra (data was not shown). The spectra of mip-RPP and mip-PP MSs are presented in Fig. 3. In comparison with mip-PP MSs, the FT-IR spectra of mip-RPP MSs shows a new peak at 1653 cm⁻¹, which is associated with the C=C stretching.[40 , 41] The change indicates the MSs generated by RPP containing some free C=C bonds on their surface, which would play an important role for the formation of monodisperse MSs, because i) these free double bonds could capturing soluble monomers and oligomers in the polymerization solution and hence increase the particle size; ii) these free double bonds would somehow prevent the polymer adhesion and aggregation.[42] As a consequence, in comparison with mip-PP MSs, the average size of mip-RPP (or mip-DPP) MSs is slightly larger (Fig. 1).

A previous work by Cleveland et al. suggested that the synthetic condition affected strongly on the status of the carboxylic acids.[43] According to their study, the IR bands around 1699 cm⁻¹ and 1736 cm⁻¹ were attributed to the carboxylic acid dimers (by hydrogen bond) and the C=O stretching of the "free" carboxy-group, respectively. It is seen in Fig. 3 that the peak intensity ratio of the hydrogen-bonded dimers to the "free" carboxylic acid on mip-RPP MSs was lower than that on mip-PP MSs. Assuming the total amount of carboxy-groups are equal on mip-RPP MSs and mip-PP MSs, the mip-RPP MSs would contain more "free" carboxylic acid, which might increase the non-specific binding of mip-RPP MSs.
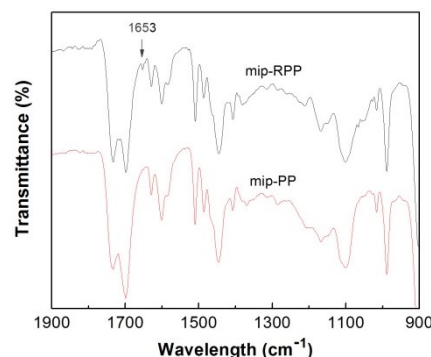

Fig. 3 FT-IR spectra of mip-RPP and mip-PP MSs.

3.2 Binding profiles of microspheres

The propranolol recognition ability of mip-RPP MSs was investigated. The binding isotherm of propranolol (from 5 μg mL⁻¹ to 300 μg mL⁻¹) on different MSs is presented in Fig. 4. For both mip-RPP and nip-RPP MSs, the binding capacity of propranolol increased linearly with the increasing of the propranolol concentration before saturated binding. Moreover, the mip-RPP MSs provide much higher (~ 5-fold) binding capacity than nip-RPP MSs in the examined concentration range. These results indicate the imprinted MSs have higher affinity to propranolol because of the interaction between the carboxyl groups in the MIPs and the amine group in propranolol. [44] As a reference, the binding profiles of propranolol on mip-PP (nip-PP) and mip-DPP (nip-DPP) MSs were also tested. We found that the binding capacity of the MSs by RPP is similar to that by PP and DPP, but slightly higher than that by PP. This might be due to the fact that the density of the "free" carboxylic acid on the MSs synthesized by RPP at high temperature is higher than that on the MSs synthesized by PP (Fig. 3).

Table 2. Freundlich isotherm equations and corresponding constants.

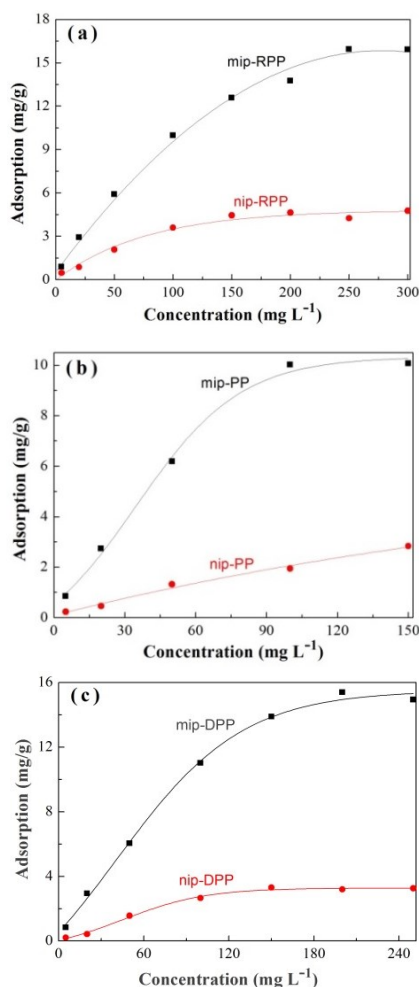| MSs	Freundlich isotherm eq	K_F	1/n	R
mip-RPP	$\ln q_e = 0.500 * \ln C_e + 0.216$	1.24	0.50	0.99
nip-RPP	$\ln q_e = 0.546 * \ln C_e - 1.356$	0.26	0.55	0.95
mip-PP	$\ln q_e = 0.545 * \ln C_e + 0.031$	1.03	0.55	0.97
nip-PP	$\ln q_e = 0.730 * \ln C_e - 2.601$	0.07	0.73	0.96
mip-DPP	$\ln q_e = 0.557 * \ln C_e + 0.085$	1.09	0.56	0.98
nip-DPP	$\ln q_e = 0.754 * \ln C_e - 2.657$	0.07	0.75	0.94

Fig. 4 Equilibrium binding profiles of propranolol on MSs by RPP (a), PP (b), and DPP (c). The MS concentration was 5 mg mL^{-1}. The samples with high propranolol concentration were diluted before testing.

According to a previous work by Umpleby II et al.,[45] the binding data of propranolol by the polymeric MSs could be further fitted to Freundlich isotherm (Fig. S3). The logarithmic form of Freundlich isotherm is given as follows:[46,47]

$$\ln q_e = \ln K_F + (1/n) \ln C_e \qquad (2)$$

where q_e is the equilibrium adsorption capacity of propranolol, C_e is the equilibrium concentration of the templates. K_F and n are the Freundlich constant related to adsorption capacity and adsorption intensity, respectively. The Freundlich constants K_F and $1/n$ were calculated and presented in Table 2. In all cases, the R values are no less than 0.94, indicating the adsorption of propranolol on MSs fits well to the Freundlich model. The constant of $1/n$ between 0.50 and 0.73 indicates favorable adsorption.[46] Moreover, the difference of K_F between MIP and NIP MSs by RPP (0.98) is identical to that by PP (0.96) and by DPP (1.02) indicating that mip-RPP MSs possess similar binding selectivity toward propranolol as that of mip-PP and mip-DPP MSs.[48]

3.3 Kinetic binding profile of propranolol

The kinetics binding of propranolol by mip-RPP and nip-RPP MSs is shown in Fig. 5a. The maximum propranolol binding by mip-RPP MSs was much higher than that by nip-RPP MSs. It is seen that the equilibrium binding time for mip-RPP and nip-RPP MSs was approximately 90 min. In the literature, propranolol binding by MIPs could be fitted to a pseudo-second-order kinetic model.[8] Here, a pseodu-second order kinetic model is also used for the simulation of the binding profiles of mip-RPP and nip-RPP MSs using the following equation:[49,50]

$$\frac{t}{q_t} = \frac{1}{K_2 q_e^2} + \frac{t}{q_e} \qquad (3)$$

where q_t and q_e are the propranolol amounts adsorbed at time t and at equilibrium, respectively, and K_2 (mg g^{-1} min^{-1}) is the rate constant of the pseudo-second-order sorption. Supposing the initial sorption rate v is $K_2 q_e^2$,[51] the constant v and q_e can be calculated by plotting t/q_t vs t (Fig. 5b). For both mip-RPP and nip-RPP MSs, the correlation coefficient (R) is higher than 0.97, indicating that the binding data are fitted well to the pseudo-second-order model. According to Fig. 5b, the q_e values for mip-RPP and nip-RPP MSs were 3.08 and 1.07 mg g^{-1}, respectively. It matched well with the binding capacities of mip-RPP and nip-RPP MSs in Fig. 4a (the data points at 20 mg L^{-1}). Meanwhile, the initial sorption rate on mip-RPP and nip-RPP MSs were 0.48 and 0.052 mg g^{-1} min^{-1}, respectively. Obviously, the larger values of q_e and v for mip-RPP MSs than that for nip-RPP MSs were originated from the creation of binding sites on the mip-RPP MSs.
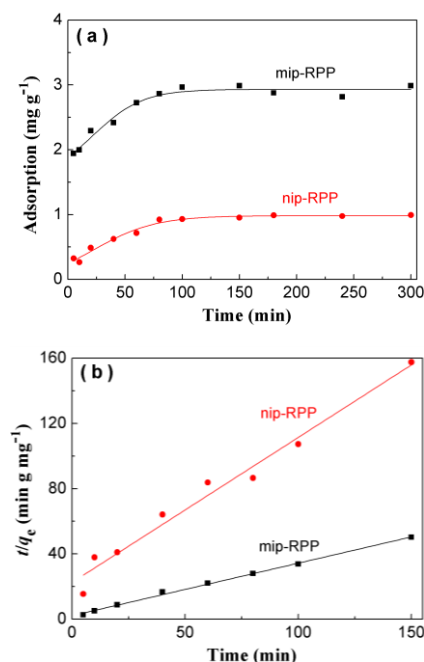

Fig. 5 (a) Kinetic binding profiles of propranolol by mip/nip-RPP MSs. (b) The simulation of the binding profiles using a Pseodu-second order kinetic model. The MS concentration was 5 mg mL^{-1}. The propranolol concentration was 67 μM (20 mg L^{-1}).

3.4 Selectivity of the mip-RPP microspheres

To investigate the selectivity of mip-RPP MSs, five compounds including propranolol, alprenolol, oxprenolol, 1-naphthylamine and 1-naphthol, possessing similar structure as indicated in Fig. S1 were selected. For propranolol, alprenolol, oxprenolol and 1-naphthylamine, the mip-RPP MSs showed higher binding capacity than the nip-RPP MSs did. The tendency of the binding difference between the mip-RPP and nip-RPP MSs was in the order propranolol > alprenolol > oxprenolol > 1-naphthylamine (Fig. 6), which may be due to the structural similarity between propranolol and the structure analogous. It is noted that 1-naphthol displayed no binding selectivity on the mip-RPP MSs, indicating that the contribution of the imprinting performance by the propanediol moiety of propranolol is much higher than that by the naphthalene ring.
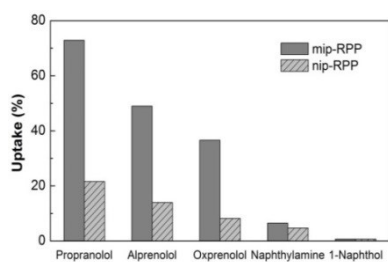

Fig. 6 Uptake of propranolol, alprenolol, oxprenolol, 1-naphthylamine and 1-naphthol by mip-RPP and nip-RPP MSs. The MS concentration was 5 mg mL^{-1}. The initial concentration of the tested substances was 67 μM for each.

To further verify the molecular selectivity of the mip-RPP MSs, the binding of the target propranolol and the interferences in a binary mixture system were also measured. In this study, oxprenolol and 1-naphthylamine were selected as the interferences. It is clear that the mip-RPP MSs showed higher binding capacity to oxprenolol than to 1-naphthylamine in the binary mixture system (Fig. 7b), which is in agreement with the observation from the single system. The selectivity was also studied by comparing the capability of displacing the template propranolol from mip-RPP MSs by oxprenolol and 1-naphthylamine. As shown in Fig. 7a, oxprenolol could displace the template binding from mip-RPP MSs, whereas 1-naphthylamine exhibited almost no effect. It is noted that the uptake of propranolol on the nip-RPP MSs in the presence of naphtheamine was slightly higher than that of single propranol (see Fig. 7a, the reason is unclear). This difference observed between oxprenolol (structural analog) and 1-naphthylamine (non-structural analog) confirms that the mip-RPP MSs containing specific binding sites.
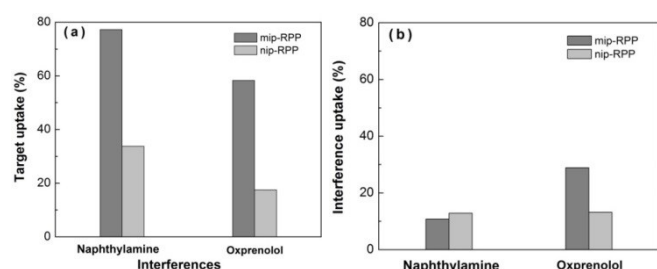

Fig. 7 Uptake of propranolol (a) and interferences (b) by the polymeric MSs in a binary mixture of propranolol with 1-naphthylamine (or oxprenolol). The

MS concentration was 5 mg mL^{-1}. The substance concentration (for both propranolol and the interferences) was 67 μM.

3.5 Effects of high temperature on molecular imprinting

Previous work shows that high temperature in DPP had no effects on the performance of propranolol-imprinted polymers.[23] However, can all the MIPs synthesized by PP (for different templates) can be successful by using DPP or RPP? To answer this question, we also prepared E2-mip-PP, E2-nip-PP, E2-mip-RPP and E2-nip-RPP MSs, respectively.

Recently, Wei et al. reported imprinted (MAA-co-DVB polymer) showed a high affinity for E2 in ACN.[52] Here, we also study E2 recognition ability of the different MSs in ACN. It is seen in Figure 8 that, E2-mip-PP shows clearly selectivity to E2, which is in agreement with the result by Wei et al. However, when PP is replaced by RPP, E2-mip-RPP and E2-nip-RPP show no different binding ability towards E2 (Fig. 8).
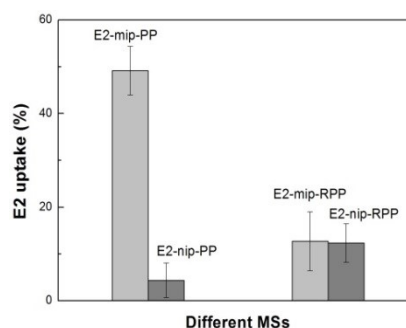

Fig. 8 Uptake of E2 by E2-mip-PP, E2-nip-PP, E2-mip-RPP and E2-nip-RPP MSs. The MS concentration was 5 mg mL^{-1}. The E2 concentration (in pure ACN) was 20 μM.

The above finding indicates that MIPs synthesized by PP (for different templates) were not always successful by using DPP or RPP. Propranolol (containing an amino group) on the template can form strong bonds with the carboxyl monomer MAA,[22] this electrostatic interactions was slightly affected by the high temperature.[53] Thus, the mip-RPP MSs could show an efficient imprinting performance. Using Theophylline (TH) as templates, we also confirmed that molecular imprinting at high temperature was highly depended on the electrostatic interactions (see Fig. S4). This finding was also supported by previous work in the literature.[17,18,22] When E2 was used as template, E2 which has two hydroxyl groups would easily form hydrogen bonds with the functional monomer MAA at low temperature.[54] However, these hydrogen bonds were strongly weakened when the temperature was increased to 90 ℃.[55] Therefore, the applicability of the DPP and RPP method is limited by the templates.

Conclusions

In this study, reflux precipitation polymerization (RPP) was used for the fabrication of MIP (mip-RPP) MSs for the first time. With this synthetic method, the monodispersed mip-RPP MSs were successfully obtained in a short time. During the

synthesis, the presence of template molecules could improve the particle morphology and size uniformity. The molecular recognition and binding selectivity were tested *via* equilibrium binding using fluorescence measurement or HPLC-UV analysis. In comparison with mip-PP and mip-DPP MSs, mip-RPP MSs showed identical selectivity. It is noted that, for the first time, we demonstrated that molecular imprinting at high temperature can be successful when electrostatic interactions played important roles in the imprinting process. On the basis of the results obtained in this study, we believe that RPP provides a new synthetic insight in molecular imprinting at high temperature. We are currently working on the development of monodispersed microgels or nanogels with high affinity for peptides and proteins using RPP and will present these in a near future.

Acknowledgment

Notes and references

1   G. Wulff, *Microchim. Acta*, 2013, **180**, 1359-1370.
2   L. Ye and K. Mosbach, *Chem. Mater.*, 2008, **20**, 859-868.
3   W. Chen, W. Lei, M. Xue, F. Xue, Z.-h. Meng, W.-b. Zhang, F. Qu and K. J. Shea, *J. Mater. Chem. A*, 2014, **2**, 7165-7169.
4   G. Vasapollo, R. D. Sole, L. Mergola, M. R. Lazzoi , A. Scardino, S. Scorrano and G. Mele, *Int. J. Mol. Sci.*, 2011, **12**, 5908-5945.
5   L. Chen, X. Wang, W. Lu, X. Wu and J. Li, *Chem. Soc. Rev.*, 2016, **45**, 2137-2211.
6   E. N. Ndunda and B. Mizaikoff, *Analyst*, 2016, **141**, 3141-3156.
7   L. Ye, *Adv. Biochem. Eng. Biotechnol.*, 2015, **150**, 1-24.
8   X. Shen and L. Ye, *Macromolecules*, 2011, **44**, 5631-5637.
9   J. Wang, P. A. G. Cormack, D. C. Sherrington and E. Khoshdel, *Angew. Chem., Int. Ed.*, 2003, **42**, 5336-5338.
10 K. Yoshimatsu, K. Reimhult, A. Krozer, K. Mosbach, K. Sode, L. Ye, B. Sellergren and K. J. Shea, *Anal. Chim. Acta.*, 2007, **584**, 112-121.
11 T. Boer, R. Mol, R. A. deZeeuw, G. J. deJong, D. C. Sherrington, P. A. G. Cormack and K. Ensing, *Electrophoresis* 2002, **23**, 1296-1300.
12 L. Surugiu, B. Danielsson, L. Ye, K. Mosbach and K. Haupt, *Anal. Chem.*, 2001, **73**, 487-491.
13 J. S. Downey, R. S. Frank, W.-H. Li and H. D. H. Stöver, *Macromolecules*, 1999, **32**, 2838-2844.
14 D. L. Murray and I. Piirma, *Macromolecules*, 1993, **26**, 5577-5586.
15 J. Jiang, Y. Zhang, X. Guo and H. Zhang, *Macromolecules*, 2011, **44**, 5893-5904.
16 X. Shen, C. Xu, K. M. A. Uddin, P.-O. Larsson and L. Ye, *J. Mater. Chem. B*, 2013, **1**, 4612-4618.
17 X. Zhang, X. He, L. Chen and Y. Zhang, *J. Mater. Chem. B*, 2014, **2**, 3254-3562.
18 J. Liu, Y. Liu, Y. Li, H. Tang and B. Wu, *Acta Polym. Sin.*, 2014, **12**, 1635-1642.
19 F. Bai, X. Yang and W. Huang, *Macromolecules*, 2004, **37**, 9746-9752.
20 J. Liu, L. Zhang, L. L. H. Song, Y. Liu, H. Tang and Y. Li, *J. Sep. Sci.*, 2015, **38**, 1172-1178.
21 J. Liu, K. Yang, Y. Qu, S. Li, Q. Wu, Z. Liang, L. Zhang and Y. Zhang, *Chem. Commun.*, 2015, **51**, 3896-3898.
22 K. Yang, M. M. Berg, C. Zhao and L. Ye, *Macromolecules*, 2009, **42**, 8739-8746.
23 C. Guo, B. Wang and J. Shan, *Chin. J. Chem.*, 2015, **33**, 225-234.
24 D. Zhao, X. Yang and W. Huang, *Polym. Int.*, 2007, **56**, 224-230.
25 Y. J. Pan, D. Li, S. Jin, C. Wei, K. Y. Wu, J. Guo and C. C. Wang, Polym. Chem., 2013, 4, 3545-3553.
26 Y. Liu, L. Wu, X. Zhao and A. Luo, *Int. J. Polym. Anal. Charact.*, 2012, **17**, 38-47.
27 C. Gou, B. Wang and J. Shan, *Chin. J. Chem.*, 2015, **33**, 225-234.
28 F. Wang, Y. Zhang, P. Yang, S. Jin, Y. Peng, J. Guo and C. Wang, *J. Mater. Chem. B*, **2014**, *2*, 2575-2582.
29 Y. Zhang, D. Li, M. Yu, W. Ma, J. Guo and C. Wang, *ACS Appl. Mater. Interfaces*, 2014, **6**, 8836-8844.
30 L. Liu, M. Yu, Y. Zhang, C. Wang and H. Lu, *ACS Appl. Mater. Interfaces*, 2014, **6**, 7823-7832.
31 Y. Chen, Z. Xiong, L. Zhang, J. Zhao, Q. Zhang, L. Peng, W. Zhang, M. Ye and H. Zou, *Nanoscale*, 2015, **7**, 3100-3108.
32 S.-D. Pan, H.-Y. Shen, L.-X. Zhou, X.-H. Chen, Y.-G. Zhao, M.-Q. Cai and M.-C. Jin, *J. Mater. Chem. A*, 2014, **2**, 15345-15356.
33 H. Sambe, K. Hoshina, R. Moaddel, I. W. Wainer and J. Haginaka. *J Chromatogr. A*, 2006, **1134**, 88-94.
34 L. Ye, R. Weiss and K. Mosbach, *Macromolecules*, 2000, **33**, 8239-8245.
35 F. Priego-Capote, L. Ye, S. Shakil, S. A. Shamsi and S. Nilsson, Anal Chem., 2008, 80, 2881-2887.
36 Y. Zhao, N. A. D. Burke and H. D. H. Stöver, *J. Polym. Sci. Part A: Polym Chem.*, 2016, **54**, 1159-1166.
37 I. Sapurina and S. Fedorova, *Langmuir*, 2003, **19**, 7413.
38 Y. Long, J. Y. Philip, K. Schillén, F. Liu and L. Ye, *J. Mol. Recognit.*, 2011, **24**, 619-630.
39 Z. Chen and L. Ye, *J. Mol. Recognit.*, 2012, **25**, 370-376.
40 G. I. Truică, N. Ditaranto, M. C. Caggiani, A. Mangone, S. C. Lițescu, E. D. Teodor, L. Sabbatini and G. L. Radu, *Chem. Pap.*, 2014, **68**, 15-21.
41 G. S. P. L. Malar and S. B. David, *Int. J. Sci. Res.*, 2015, **4**, 1960-1964.
42 L. Barner, C. Li, X. Hao, M. H. Stenzel, C. Barner-Kowollik and T. P. Davis, *J. Polym. Sci. Part A: Polym Chem.*, 2004, **42**, 5067-5076.
43 C.S. Cleveland, S.P. Fearnley, Y. Hu, M.E. Wagman, P.C. Painter and M.M. Coleman, *J. Macromol. Sci.: Phys. B*, 2000, **39**, 197-223.
44 J. Haginaka and Y. Sakai, *J. Pharm. Biomed. Anal.*, 2000, **22**, 899-907.
45 R. J Umpleby II, S. C Baxter, M. Bode, J. K Berch Jr., R. N Shah and K. D Shimizu, *Anal. Chim. Acta*, **2001**, 435, 35-42.
46 X. Shen, L. Zhu, G. Liu, H. Hu and H. Tang, *Environ. Sci. Technol.*, 2008, **42**, 1687-1692.
47 R. J. Umpleby, S. C. Baxter, Y. Chen, R. N. Shah and K. D. Shimizu, *Anal. Chem.*, 2001, **73**, 4584-4591.
48 G. T. Rushton, C. L. Karns and K. D. Shimizu, *Anal. Chim. Acta*, 2005, **528**, 107-113.
49 Y. Liu, J. Gao, C. Li, J. Pan, Y. Yan and J. Xie, *Chin. J. Chem.*, 2010, **28**, 548-554.
50 C. Dai, J. Zhang, Y. Zhang, X. Zhou and S. Liu, *Plos one*, 2013, **8**, e78167.

51 H. Surikumaran, S. Mohamad and N. M. Sarih, *Int. J. Mol. Sci.*, 2014, **15**, 6111-6136.
52 S. Wei, A. Molinelli and B. Mizaikoff, *Biosens. Bioelectron.*, 2006, **21**, 1943-1951.
53 S. S. Shah, N. U. Jamroz and Q. M Sharif, *Colloids and Surfaces A: Physicochem. Eng. Aspects*, 2001, **178**, 199-206.
54 H. Dong, A.-j. Tong and L.-d. Li, *Spectrochim. Acta A*, 2003, **59**, 279-284.
55 M. M. Coleman, K. H. Lee, D. J. Skrovanek, and P. C. Painter, *Macromolecules*, 1986, **19**, 2149-2157.